



Journal of Mining and Environment (JME)

journal homepage: [www.jme.shahroodut.ac.ir](http://www.jme.shahroodut.ac.ir)



## An Analytical Method of Predicting Length of Grout Penetration in Jointed Rocks

Mohammad Mahdi Nazempour and Abbas Majdi\*

School of Mining Engineering, College of Engineering, University of Tehran, Tehran, Iran

### Article Info

Received 12 October 2021

Received in Revised form 12 December 2021

Accepted 30 December 2021

Published online 30 December 2021

DOI:10.22044/jme.2022.11435.2127

### Keywords

Jointed rocks

Rock joints

Newton's second law

Binghamian fluid

Length of grout penetration

### Abstract

Prediction of the length of grout penetration and assessment of the groutability around the boreholes in the jointed rocks have a crucial effect on the planning and execution of grouting. Grout distribution in jointed rocks is a function of the geo-mechanical properties of rock mass, grout properties, and grout operational performance. This paper describes an analytical model based on the Newton's second law, with the assumption of disk-shape model for the joints in order to calculate the maximum length of grout penetration in the horizontal and angled joints. It is shown that the proposed formulas can predict the length of grout penetration in rock masses with numerous joint sets as well. In order to validate the proposed model, it is compared with the existing analytical and empirical criteria, showing a very good accordance with their calculated results. Finally, the proposed analytical model is used to design the grout planning of a water conveying tunnel that is subjected to a heavy inflow. The design results in a successful filling of the vacant space behind the segmental lining and sealing the tunnel to stop the inrush water. These show that the model proposed in this paper can be successfully applied in practice.

## 1. Introduction

Grouting is the process of injecting a grout compound into the empty spaces of the host rock mass to improve the engineering properties of the rocks for the short- and long-term purposes. The grouting operation has become a crucial part of many civil and mining engineering projects. During the investigations related to grout distribution and improvement of the rock behavior caused by grouting, the length of grout penetration is of the outmost important. Generally, joint aperture, grouting pressure, and grout mixture's properties are the main parameters influencing the grout penetration in rock masses.

Indeed, the joints and fractures of rock masses are the controlling factors of grout flow due to negligible penetration in voids of most rocks. In the recent decades, it has become clear that the fluid flow in rock masses under the ground surface mainly occurs inside the fractures [1]. Ideally, the

joints are supposed as two smooth, parallel planes. Natural joints, however, have rough surfaces and variable apertures so the equivalent aperture through which the fluid can flow is smaller than what is measured in the field [2-7]. The grouting pressure is the major effective parameter in a grouting operation. It is usually perceived that the maximum penetration length is achieved as a result of applying the maximum pressure, and yet the maximum safe pressure should always be applied [8]. One of the most important parameters of the grout is its viscosity that slowly increases during preparation, and rapidly increases in the course of grouting. The initial viscosity is dependent on the grout composition, chosen according to the circumstances of the ground and the purpose of the operation. The interaction between the cement particles when water is added creates a network structure, which results in a non-linear relation



Corresponding author: [amajdi@ut.ac.ir](mailto:amajdi@ut.ac.ir) (A. Majdi).

between the shear stress and shear rate, i.e. thixotropic behavior, which has to be overcome for flow initiation. This parameter, known as yield stress, has a noticeable effect on grout penetration in the joints. It is vital to know the way the grout propagates in the joints in order to understand its propagation in the whole rock mass, followed by assessment of its influence on the rock mass properties. Considering this, different researchers have suggested both analytical and empirical formulas for calculation of radius of grout penetration in the joints [9-15], which are presented in Table 1.

Due to the complexity of the factors impacting the grouting and uncertainties in rock masses [16-19], some researchers have used physical modeling for the investigation of grout propagation in rock fractures. Based on radial flow towards the outside of the grout, Nonveiller [19] has developed a test tool to measure the necessary grouting pressure for grouting of joints intersecting the borehole during the gelation time and only for low pressures. Verfel [20] has presented a report on a test set with a pre-determined distance for a radial flow. The assumed distance was small enough but able to be grouted. Afterwards, a canal-shaped test tool was suggested for determination of the initial grouting pressure [15]. Draganovic and Stille [21] have developed a model with a small gap between two assembled disks with clamps with the intention of studying the filtration and cementitious length of grout penetration. The physical modeling tools have been suggested as well [22]. In general, most of the experimental models were as two parallel planes with smooth surfaces.

The principal aspects of Newtonian fluid flow (such as underground water) in canal structures that are dominant in geological formations have been studied both in two dimensions [23-25] and three dimensions [26-28]. However, cementitious grouts, which are usually used in engineering projects, are mostly non-Newtonian fluids [9, 29-33]. Only if the shear stress exceeds the yield stress, then the cementitious grouts will start to flow. Most of the non-Newtonian fluids show a non-linear rheological behavior, generally known as the Herschel-Bulkley model [34]. This model consists of three parameters: yield stress, consistency index,  $k$ , and fluid index,  $n$ . Selection of the specific parameters decreases the model to the Binghamian model, power law or Newtonian models, respectively. The experimental studies have shown that cementitious grouts with water to cement ratio (w:c) between 0.6 and 0.8 are actually yield power law fluids [30, 32, 33, 35]. Some

special grouts such as fine cementitious grouts with high water to cement ratio,  $w:c \geq 1$ , are cementitious grouts modified by polymer and silica sol, Newtonian or power law fluids [36].

The length of grout penetration is clearly an important parameter for the assessment of the efficiency of a grouting operation. As well as this, it determines the extent of reinforcement occurred in rock masses [37-40]. Hässler *et al.* [39] and Eriksson *et al.* [41] have used a 1D pipe network model in order to study the flow in the fracture networks with constant aperture. The very elementary models of grout propagation applied parallel planes to describe the fractures. Such models always produce symmetrical patterns of grout propagation. The advantages of these models are relative simplicity and having analytical solutions for time-related flows of non-Newtonian fluids.

Modification of grouting based on the model of Hässler *et al.* was made by Janson [42] and Dalmalm [43, 44]. The 1D fracture models were then developed to 2D fracture networks [45, 46].

As mentioned earlier, in many cases, cement grouts show the Binghamian fluid behavior. Numerous analytical solutions have been proposed for the Binghamian fluids. Based on the solutions of Hässler *et al.* [40, 47], Gustafson *et al.* [48] have presented a theoretical solution to grouting time as a function of grout penetration assuming that both the pump and underground water pressures were constant, grout properties were time-independent and neglecting the underground water, and proposed a stop criterion using the minimum grouting time to replace the conventional criteria based on the flow rate or total flow of grout. These analytical methods provided the theoretical basis for Real Time Grouting Control (RTGC) [49-51]. A penetrability algorithm based on an explicit grouting pressure algorithm for rock mass fracture has been presented in order to model the process precisely and efficiently [40]. Based on the truncated power law fluid and Binghamian fluid, numerous models have been proposed for numerical modeling of grout flow in a porous medium and rock fracture with rough walls (e.g. [52-54]). Amadei and Savage [55] have suggested an analytical solution for visco-plastic Binghamian materials, which may be helpful to understand the grout flow process in rock fractures. Considering the fact that most of these solutions are non-linear, tough equations, computer and numerical methods are applied to solve them. Yang *et al.* [56] have developed a numerical model based on the random joint network to model the Binghamian grout

penetration in fractured rock masses. Mortazavi and Maadikhah [57] and Fidelibus and Lenti [58] have conducted numerical studies on the important factors controlling the grout flow in rock masses.

Some researchers have studied hydro-mechanical coupling in rock fractures [59-62]. Several numerical methods have been proposed for the simulation of hydro-mechanical coupling [63-68]. The effect of fracture deformation during the grouting process has been the topic of investigation done by the other researchers [69-71]. Another research work [72] has shown that if hydro-mechanical coupling is considered, the aperture of larger joints will increase with grouting pressure increase, and the aperture of smaller joints will

decrease due to joint interaction, resulting in a decrease in the penetration length in the latter joints. This was in contrast with the prevalent belief that claimed that the higher the pressure, the greater the length of penetration in small joints. Furthermore, a high grouting pressure can increase the risk of rock jacking and high cost [73-75]. These studies, have highlighted the necessity of a safe grouting pressure. As well as this, the influence of critical shear rate on the grout penetration has been studied [76]. In great depths, a grouting pressure equal to two times the underground water has been reported to help reach the required length of penetration [77, 78].

**Table 1. Equations proposed by different researchers for calculating length of grout penetration in rock joints.**

Reference	Year	Equations	Descriptions
Wittke [9]	1968	$R = \frac{a \times P}{\tau_0} + r$	Rock Joint was modeled as a pipe.
Wittke [10]	1990	$R_g = \frac{\frac{b \times P_g}{2\tau_g} + r_g}{1 + \frac{b}{2\tau_g}(\gamma_g - \gamma_w) \sin \alpha \sin \varphi}$	Rock joint was modeled as an elliptical disk.
Jiacai <i>et al.</i> [11]	1982	$t_g = \frac{1.02 \times 10^{-7} \times \mu_g (R_g^2 - r_0^2) \log \left( \frac{R_g}{r_0} \right)}{P_g \times w^2}$	Time was entered in the formula.
Lombardi [12]	1985	$R_{max} = \frac{P_{max} \times t}{C}$	This formula is the simplified form of Wittke's formula.
Lau and Crawford [13]	1986	$R = \left[ \frac{P \times b \times D}{\tau_0} + \frac{D^2}{4} \right]^{1/2} - \frac{D}{2}$	This formula was obtained based on penetration of cement grout between two glass plates.
Shroff and Shah [14]	1999	$R_g = \frac{I}{n l w}$ $w^2 = 3.46 \times n \times l \times \sqrt{\frac{\mu_g - \mu_w}{P_g}} \times \sqrt{Q_g \times l}$	This equation includes the number of joints.
Majdi <i>et al.</i> [15]	2004	$R_{gj} = \left[ \frac{\mu_w}{\mu_g} \right] \times \left[ \frac{W}{H_j} \right] \times \left[ \frac{P_g}{\gamma_g} \right] \times \left[ \frac{P_g \times t_g}{\mu_g} \right]^c$	This equation was obtained from dimensional analysis.

$R_g$ : length of grout penetration,  $r_0$ : borehole radius,  $w$ : joint aperture,  $P_g$ : grouting pressure,  $\tau_0$ : yield stress,  $\gamma_g$ : specific gravity of grout,  $\gamma_w$ : specific gravity of water,  $\mu_g$ : viscosity of grout,  $\mu_w$ : viscosity of water,  $l$ : length of the intersection of joint and borehole,  $n$ : number of joints intersecting the borehole,  $Q_g$ : flow rate,  $I$ : volume of grout,  $\varphi$ : angle defined on ellipse plane of penetration,  $\alpha$ : angle of joint with horizontal plane,  $t_g$ : grouting time.

Liu *et al.* [79] conducted a research work on the effect of *in situ* stress on the joint aperture and the length of penetration in fracture networks. The results obtained showed that the penetration lengths near the isotropic ones were observed in the cases with lower *in situ* stress ratio, while the

fractured rocks in the critical stress states showed extremely anisotropic penetration lengths. Grouts tend to concentrate in the fractures with larger apertures under a critical stress so the length of penetration would be greater in them. In practice, the borehole density in the same direction of

maximum stress is smaller since the length of penetration is greater in this direction.

The effect of underground water on the length of penetration in rock fractures and the necessity of taking it into consideration has been studied [80]. In another research work [81], it has been shown that with yield stress increasing, the length of penetration decreases substantially. Also the abnormalities in the joint aperture can have a huge bearing on the grout propagation. Lee *et al.* [82] have conducted an experimental study on the penetration grouting distribution around a tunnel. In this research work, a test tool was made using the umbrella method in order to simulate penetration of grouting around the tunnels. The distribution of the grout around a tunnel model and an artificial joint with adjustable aperture caused by applying given pressures, showing a direct relation between the joint aperture and the length of penetration.

Wang *et al.* [83] have carried out experimental tests to study the effect of fracture roughness on the grout penetration, and the impact of grout speed on water bleeding. Shamu *et al.* [84] have proposed suggestions for the use of shear rate in the grouting design, presenting a nomogram to compute the key parameters for the practical purposes. Rafi and Stille [85] have proposed an analytical approach to define stop criteria that allow the spread of grout to a certain distance, while controlling deformations to the extent that ensures fracture jacking that ensures fracture jacking remains beneficial.

All these studies show that the grout propagation in rock joints and prediction of penetration length have been the topic of many investigations. With regard to the grouting design, it is beneficial to have an accurate assessment of the length of grout penetration in order to design the suitable distance between the grouting boreholes and predict the grout volume. In addition, aside some genuine limitations, the mathematical models are of paramount significance due to their stronger theory and more simple application. If they are based on a correct basis, these models are beneficial in that they can give quantities with an appropriate accuracy. Therefore, in this work, equations for calculation of the length of grout penetration in joints are presented, based on which a criterion is proposed for consideration of the length of grout penetration in rock mass.

## 2. Assumptions of problem

Generally, the factors affecting the length of grout penetration in rocks can be classified as: 1)

Rock joints characteristics such as aperture and roughness, 2) technical factors, among which the grouting pressure is the most important one, 3) grout properties including viscosity and cohesion. With the diversity of the properties and the large discrepancy of these factors taken into consideration, an analytical model for calculating the length of grout penetration is generally hard to achieve, and its application might be followed by some errors. Consequently, the mathematical models have to be based on a realistic basis. In this paper, the assumptions made are as follow:

- 1) The joint is assumed as a planar structure with infinite length and width and finite and constant aperture.
- 2) The particles' size suspended in cement grout is very small compared to the joint aperture (the groutability ratio is very high).
- 3) Grout distribution occurs in the form of a disk in the joint plane.
- 4) The joint surfaces are smooth, without curvature, and there is no filling inside the joint.
- 5) During the grouting process, there will be no change in the nature of the joint, and it will not undergo any deformation.
- 6) The grout is incompressible, and will not reach its setting time.
- 7) Capillary effects are ignored.
- 8) The fluid flow is linear.
- 9) The joint aperture is much smaller than the lateral dimensions.
- 10) The grout fluid is Binghamian. Nevertheless, for simplicity and the possibility of presenting an explicit equation, it is assumed that the fluid velocity profile is parabolic.

## 3. Scientific basis of problem

During the grouting process, what causes the grout to move along the joint is the force applied by the pump. Therefore, the force that is applied in the opposite direction of grout movement and finally makes the grout stop is the friction force between the joint walls and the grout. Basically, at the maximum pressure, when the grout does not penetrate the joint anymore, the backlash state will happen. This occurs when the maximum length of penetration is reached. At this point, the force created by the shear stress at the joint wall reaches its peak. As a result, the pump force will not be able to move the grout. In other words, movement and stop of the grout depend on the bilateral performance of these two force on the fluid. In

addition, the Binghamian fluids will not start to move until an external force is applied. From this viewpoint, they have a similar behavior to that of solids. As a result, the best but simplest tool that can model the grout movement is the Newton's second law, which is based on a strong physical basis, and has been widely used in fluid mechanics.

#### 4. penetration in a horizontal joint

In practice, it is not intended to grout a single joint. However, grout propagation in a joint is the basis of rock mass grouting. According to the assumptions of the problem, the joint geometry and grout distribution are shown in Figure 1. In this case, it is assumed that the joint is located in the horizontal plane, and the borehole has been perpendicular to the center of the plane.

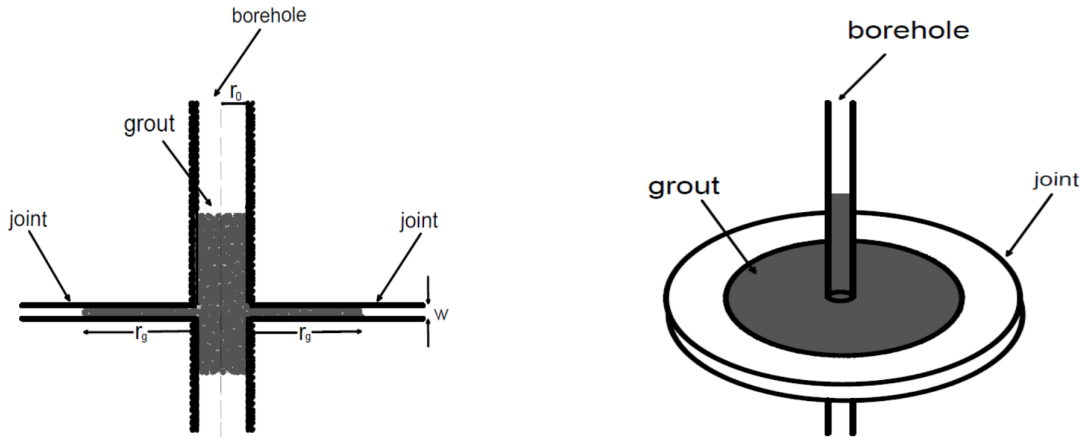


Figure 1. Schematic depiction of geometrical mode of the joint and grout propagation inside the joint.  $w$ : joint aperture,  $r_0$ : borehole radius,  $r_g$ : maximum length of grout penetration.

The general form of the Newton's second law is:

$$\sum F = ma \tag{1}$$

In this formula,  $\sum F$  is the resultant force,  $m$  is the mass, and  $a$  is the acceleration of the matter caused by the resultant force. In a horizontal joint, the force applied on the grout is the force applied by the pump ( $F_p$ ), and that resulted from the friction between the grout and the joint walls ( $F_\tau$ ). Thus:

$$\sum F = F_p - F_\tau \tag{2}$$

The pump force can be calculated using the following formula:

$$F_p = 2\pi r_0 w P_p \tag{3}$$

where  $r_0$  is the borehole radius and  $w$  is the joint aperture. In order to calculate the shear force exerted on the grout, it is necessary to determine the shear stress distribution along the joint. The yield stress is the minimum stress that has to be applied on the fluid to make it move. The grouting pressures are always greater than the yield stress so the shear stress will be greater than the yield stress. This highlights the necessity of determination of shear stress distribution along the joint, which, in

turn, is vital for calculation of the shear force exerted on the grout. The shear stress in the Binghamian fluids can be defined as:

$$\tau_r = \tau_0 + \mu_g \dot{\gamma} \tag{4}$$

in which  $\tau_r$  is the shear stress,  $\tau_0$  is the yield stress,  $\mu_g$  is the grout viscosity, and  $\dot{\gamma}$  is the parameter that is known as the shear strain rate or shear velocity. If the axis perpendicular to the joint (parallel to the borehole) is  $z$ -axis, the shear strain rate equals:

$$\dot{\gamma} = \frac{\partial^2 u}{\partial z \partial t} = \frac{\partial \dot{u}}{\partial z} = \frac{dv}{dz} \tag{5}$$

in which  $v$  is the grout velocity inside the joint.

It is clear that as the grout propagates inside the joint, the shear force will increase due to the considerable increase of  $A_n$ . This is the factor that finally makes the grout stop. With this in mind, the shear force can be calculated as:

$$F_\tau = 2 \int_{r_0}^r \tau_r(r) dA_t \tag{6}$$

in which  $\tau_r(r)$  is the shear stress distribution along the joint and  $dA_t$  is the element of joint surface area on which the grout is in contact with one joint wall.

In order to calculate  $\frac{dv}{dz}$ , the velocity distribution of grout inside the joint has to be determined first. Since the grout shows a Binghamian behavior, the velocity profile is as illustrated in Figure 2. As it can be seen, there is a region in the central part of the profile called the plug area. For simplicity, in the present work it is assumed that the velocity profile would be a complete parabola (similar to

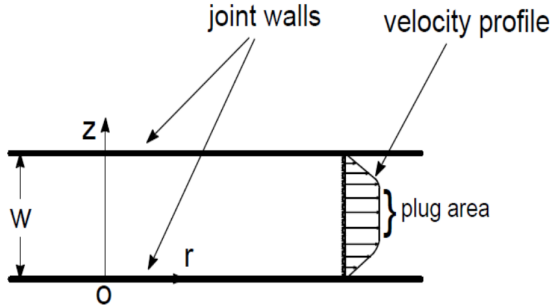


Figure 2. Approximate profile of a Binghamian fluid velocity inside a joint.

According to Figure 3, the velocity equation can be expressed as:

$$v(z) = \left(-\frac{4v_{\max}}{w^2}\right)z^2 + \left(\frac{4v_{\max}}{w}\right)z \quad (7)$$

Therefore, the shear strain rate will turn into:

$$\frac{dv}{dz} = \frac{4v_{\max}}{w} \quad (8)$$

$v_{\max}$ , which is the maximum velocity of the fluid, can be obtained from the average velocity,  $v_{\text{ave}}$  [47]. The average velocity can be calculated from the following formula:

$$v_{\text{ave}} = \frac{Q_g}{A_n} = \frac{Q_g}{2\pi r w} \quad (9)$$

where  $Q_g$  is the flow rate. Therefore, the shear stress is obtained as:

$$\tau_r(r) = \tau_0 + \frac{6\mu_g Q_g}{2\pi r w^2} \quad (10)$$

As a result, from Equation (6), the shear force can be expressed as:

$$F_\tau = (2\pi\tau_0)(r^2 - r_0^2) + \left(\frac{12\mu_g Q_g}{w^2}\right)(r - r_0) \quad (11)$$

The grout acceleration can be ignored due to its small quantity, so Equation (1) turns into:

$$(2\pi r_0 w P_p) = (2\pi\tau_0)(r^2 - r_0^2) + \left(\frac{12\mu_g Q_g}{w^2}\right)(r - r_0) \quad (12)$$

Equation (12) is a quadratic equation, thus having two roots, and only the positive root is acceptable here. With this taken into account, the

the Newtonian fluids), as shown in Figure 3. Since the average velocity is to be used in the present research work, the resultant forces will be calculated on the joint surface, and the length of penetration determines a point on the joint surface. This simplification is logical, and the results obtained will be very near to the reality. This helps the equations to be explicit and more user-friendly.

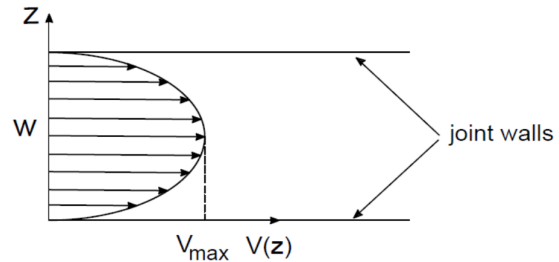


Figure 3. Approximate profile of a Newtonian fluid inside a joint.

maximum length of grout penetration can be calculated from Equation (13):

$$r_g = \frac{-(B) + \sqrt{[(B)^2 + 4D(C + Dr_0^2 + Br_0)]}}{2D} \quad (13)$$

in which:

$$B = \frac{12\mu_g Q_g}{w^2}$$

$$C = 2\pi r_0 w P_p$$

$$D = 2\pi\tau_0$$

The units of all parameters included in equation (14) are according to the SI system. The joint aperture is an important parameter affecting the length of grout penetration in rock joints. According to the fact that natural joints occur with a wide range of apertures, the ISRM classification for joints [86] is used in the present work, which is shown in Table 2.

Table 2. Classification for description of rock fractures according to ISRM [86].

Fracture condition	Description	Aperture	
Closed fractures	Completely closed	<0.1	mm
	Closed	0.1-0.25	mm
	Almost closed	0.25-0.5	mm
Open fractures	A little open	0.5-2.5	mm
	Almost open	2.5-10	mm
	Open	>10	mm
Very open fractures	Very open	1-10	cm
	Highly open	10-100	cm
	Cave-shaped	>100	cm

The length of grout penetration was calculated for different joint aperture quantities in the range of 0.1 mm to 10 cm, and grouts with water to cement

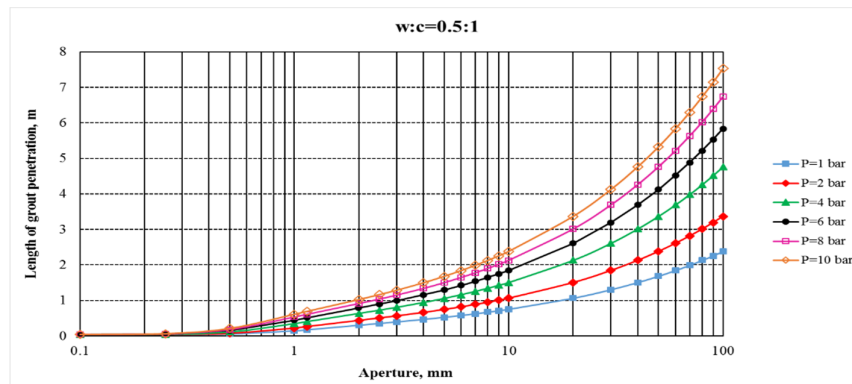
ratios of 0.5:1, 1:1, and 2:1. The fluid properties and technical properties used in the calculations are presented in Table 3.

**Table 3. Grout properties and technical properties used in calculation of length of grout penetration (derived from [14] and [87]).**

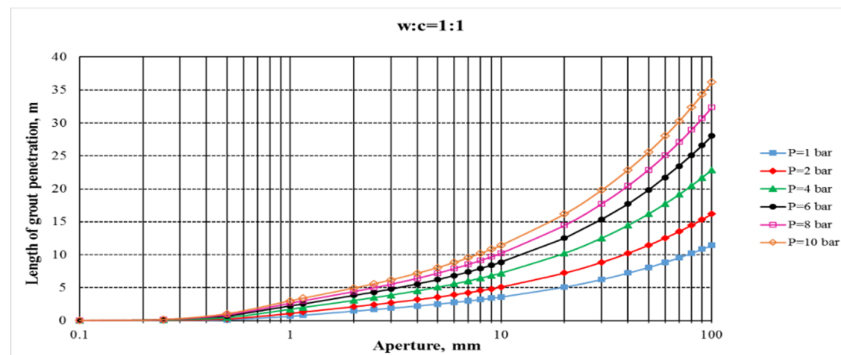
Parameter	w:c = 0.5:1	w:c = 1:1	w:c = 2:1
Specific gravity (kg/m <sup>3</sup> )	1840	1520	1290
Viscosity (Poise)	0.37	0.06	0.025
Yield stress (Pa)	67	2.9	1
Flow rate (L/min)	20	20	20
Borehole diameter (mm)	76	76	76

Figure 4 shows the length of grout penetration for a grout with water to cement ratio of 0.5:1 and the grouting pressures of 1, 2, 4, 6, 8, and 10 bar.

Figure 5 shows the length of grout penetration for a grout with the water to cement ratio of 1:1, and Figure 6 shows it for a grout with the ratio of 2:1.



**Figure 4. Length of grout penetration for a cement grout with w:c = 0.5:1 versus joint hydraulic aperture.**



**Figure 5. Length of grout penetration for a cement grout with w:c = 1:1 versus joint hydraulic aperture.**

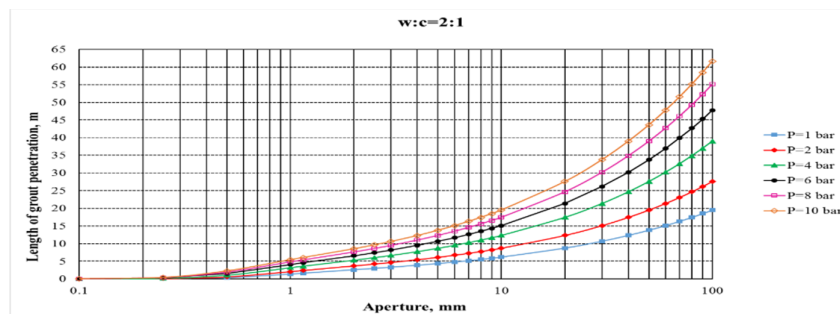


**Figure 6. Length of grout penetration for a cement grout with w:c = 2:1 versus joint hydraulic aperture.**

**5. Length of grout penetration in an angled joint**

Since many natural joints are angled, an equation for calculation of the length of grout penetration in these joints seem to be vital. The distinctive factor in his case is the gravity force, which impacts grout propagation. Assumptions in this section will be similar to those of the horizontal case. It is assumed that the joint plane is located at an angle of  $\alpha$  with respect to the horizontal plane. Besides, the borehole is considered to be drilled in the center of the joint plane intersecting it at an angle of  $90-\alpha$ . Due to the exertion of gravity force, the grout distribution in the joint plane will be in the form of an ellipse. Figure 7 shows the geometry of the problem.  $\theta$  is the angle of different positions on the

joint plane with respect to the major diameter of the ellipse.

The equation of the equilibrium of the forces is in the form of:

$$\sum F = F_p - F_\tau - F_g = 0 \tag{14}$$

in which  $F_g$  is the force resulting from the weight of the grout in the joint, and can be calculated from the following equation [88]:

$$F_g = 2\pi\rho_g g w r_0 (r_g - r_0) \cos \theta \sin \alpha \tag{15}$$

$F_p$  and  $F_\tau$  can be calculated from Equations (3) and (11), respectively. Hence, maximum length of grout penetration for different locations in an angled joint can be calculated as:

$$r_g = \frac{-(B + E) + \sqrt{[(B + E)^2 + 4D(C + Dr_0^2 + (B + E)r_0)]}}{2D} \tag{16}$$

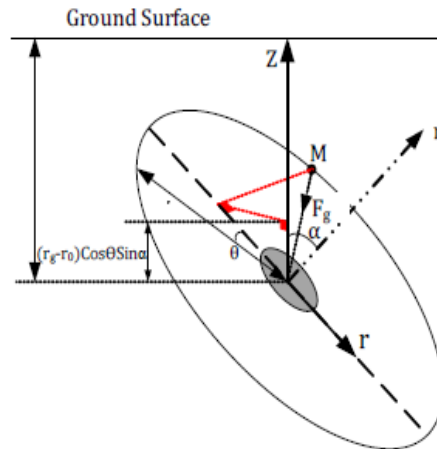
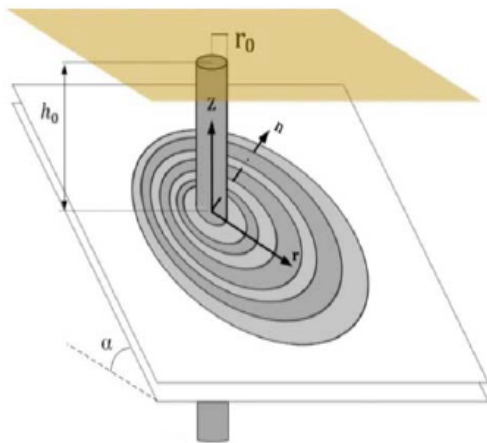


**Figure 7. A schematic depiction of geometry of an angled joint and grout propagation in it [88].**

in which:

$$B = \frac{12\mu_g Q_g}{w^2}$$

$$C = 2\pi r_0 w P_p$$

$$D = 2\pi\tau_0$$

$$E = 2\pi\rho_g g w r_0 \cos \theta \sin \alpha$$

In order to check the accuracy of the equation, if  $\alpha = 0$  in Equation (17), Equation (14) can be obtained, which calculates the length of penetration in a horizontal joint.

Since the length of penetration in the upper part of the joint is smaller than that in the lower part due

to gravity force exertion, calculations are made for the case of  $\theta = 0$ . Figures 8 and 9 illustrate the changes in the length of grout penetration of joints with different angles with respect to the horizontal plane for the joint apertures of 2.5 mm and 10 mm, respectively, for a grout with water to cement ratio of 0.5:1. Figures 10 and 11 show the changes in the length of penetration for a fluid with a ratio of 1:1, and Figures 12 and 13 depict the changes in the length of grout penetration for a fluid with water to a cement ratio of 2:1. As expected, the length of penetration decreases in the upper part of the joint as  $\alpha$  increases. This can be ascribed to the gravity force. Thus when designing the boreholes and predicting the distance between them, it is vital that we consider the length of penetration in the upper part of the joint.

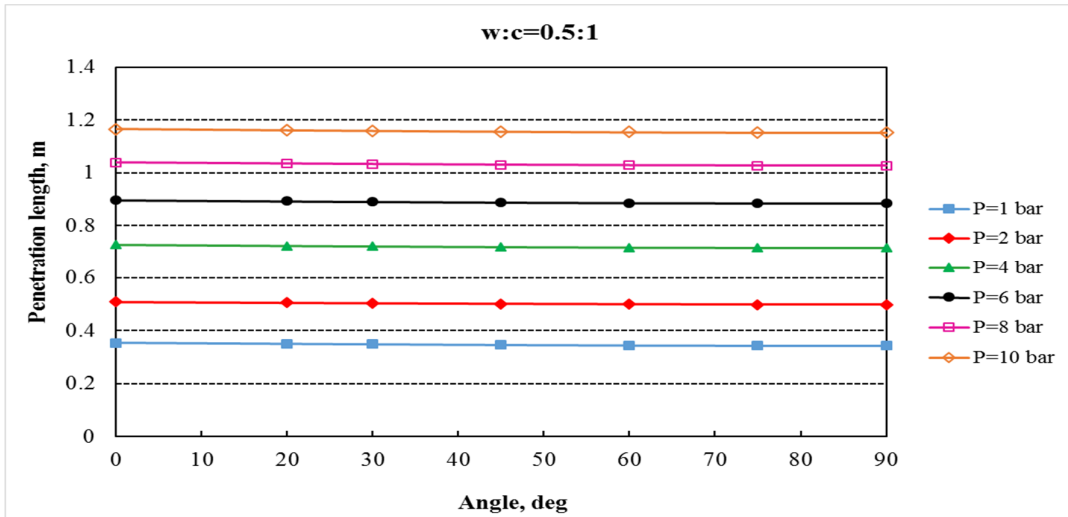


Figure 8. Length of grout penetration for upper part ( $\theta = 0$ ) of an angled joint with hydraulic aperture of 2.5 mm and a grout with w:c = 0.5:1.

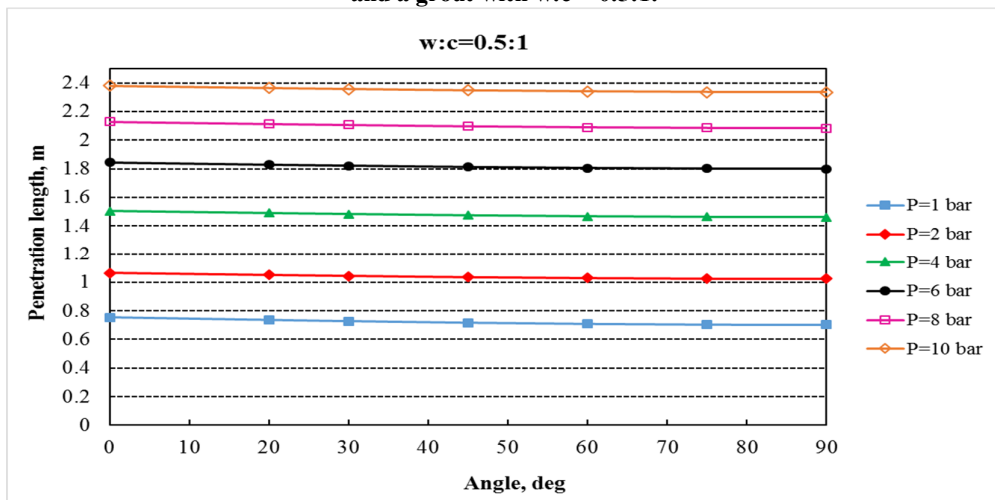


Figure 9. Length of grout penetration for upper part ( $\theta = 0$ ) of an angled joint with a hydraulic aperture of 10 mm and a grout with w:c = 0.5:1.

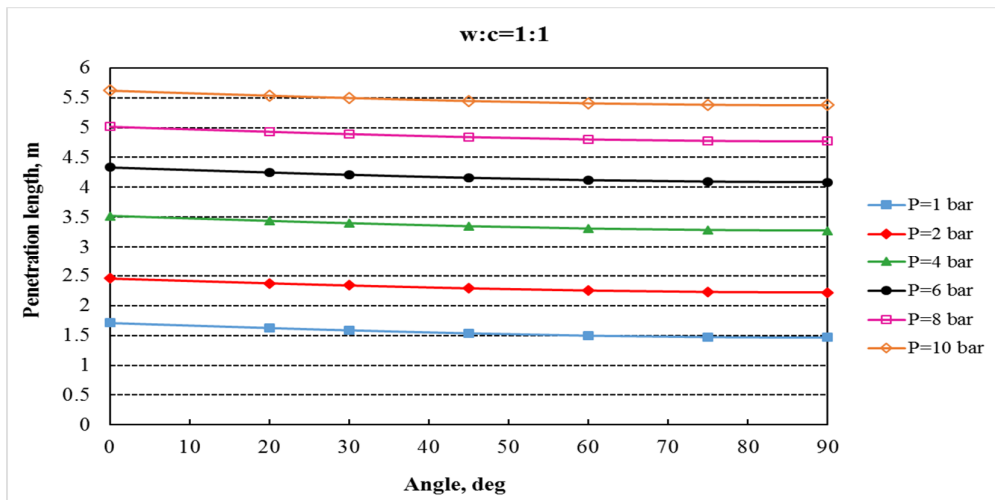


Figure 10. Length of grout penetration for upper part ( $\theta = 0$ ) of an angled joint with a hydraulic aperture of 2.5 mm and a grout with w:c = 1:1.

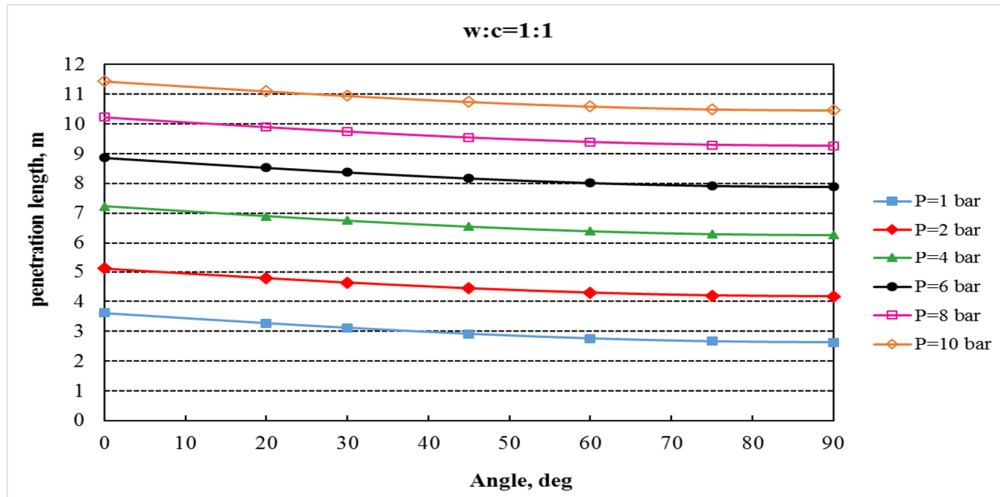


Figure 11. Length of grout penetration for upper part ( $\theta = 0$ ) of an angled joint with a hydraulic aperture of 10 mm and a grout with w:c = 1:1.

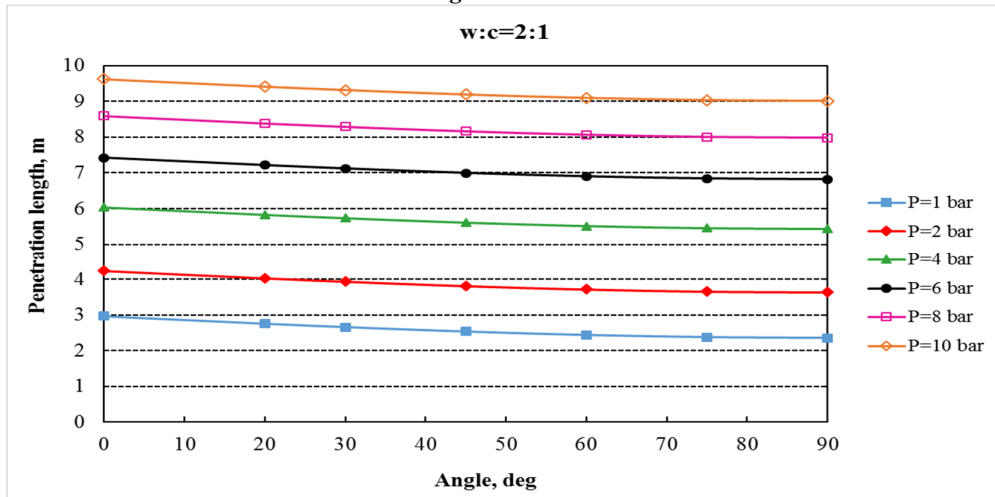


Figure 12. Length of grout penetration for upper part ( $\theta = 0$ ) of an angled joint with a hydraulic aperture of 2.5 mm and a grout with w:c = 2:1.

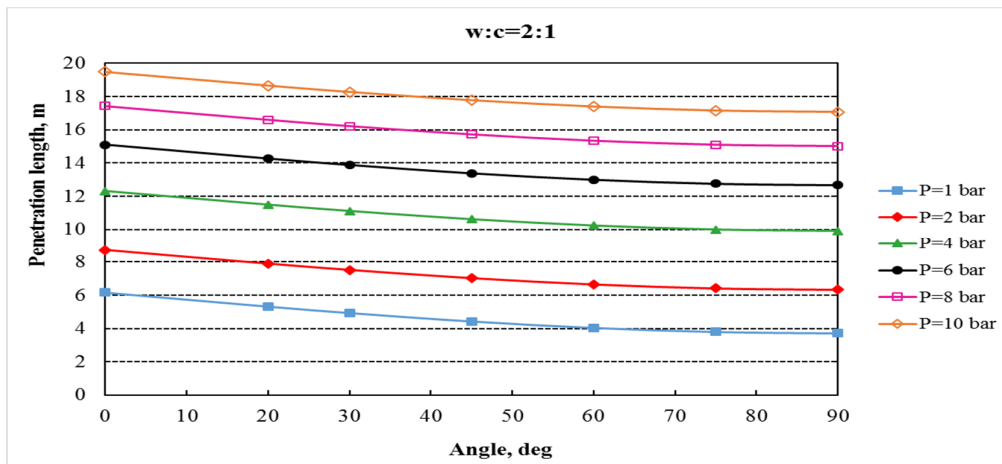


Figure 13. Length of grout penetration for upper part ( $\theta = 0$ ) of an angled joint with a hydraulic aperture of 10 mm and a grout with w:c = 2:1.

## 6. Grouting of a rock mass with multiple joints

Hardly ever do single joints occur in the nature. As a result, the designers usually deal with the joint sets, and they almost always intent to grout rock masses. In each joint set, the joint properties including aperture, spacing, and persistence can

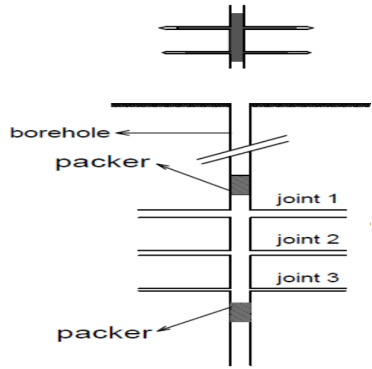


Figure 14. Grouting a rock mass with horizontal joints.

Firstly, the grouting process is going to be described for one horizontal joint set. Then it will be developed for the general case of multiple joint sets.

It is assumed that  $n$  horizontal joints of a set are intersected by the borehole. This section is separated by packers from the other parts of the borehole. Figure 16a shows the configuration of joints and grouting packers. The grouting operation starts with regulating a flow rate of  $Q$  and a grouting pressure of  $P_p$  on the pump. The pressure equals zero initially. The grout enters the borehole with a constant flow rate of  $Q$ , and starts to fill the borehole from the lower part of the section until it reaches the first joint ( $j_1$ ), enters  $j_1$  and continues to propagate inside it. Simultaneously, the fluid goes up inside the borehole, and when reaching  $j_2$ , the grout propagates in it too (Figure 16b). This process goes on until the grout arrives at  $j_n$  (Figure 16c), followed by filling of the section totally. Afterwards, the pump pressure increases gradually, and finally it reaches the maximum pre-determined value of  $P_p$ . At this step, the grout is propagating in all joints such that the length of penetration is greater in the lower joints.  $j_1$  is the first joint in which the maximum length of penetration,  $r_g$ , is reached, which can be calculated using Equation (14). Figure 16d shows this step of the process.

Having reached its maximum length of penetration in  $j_1$ , the grout is stopped in this joint, backlashes, and the fluid penetrates the other joints

change in a limited range. Generally, the joints may occur with various apertures (Figure 14).

Rock masses may contain joint sets in different directions, and this can cause complications in the projects practically. The ideal condition is to grout the intended area of the rock mass both completely and properly. Figure 15 depicts an ideal grouting in a rock mass with multiple joint sets.

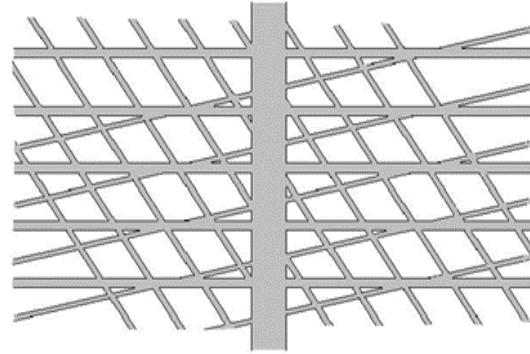


Figure 15. Ideal grouting of a rock mass with multiple joint sets.

with a flow rate of  $Q$  (Figure 16e). The locations of the grout in joints  $j_1$  to  $j_n$ , if connected to each other, produce a space with curved lateral surface, whose 2-d projection is illustrated in Figures 16d and 16e. In the present work, it is assumed that the viscosity and yield stress of the grout will remain constant, allowing the process to continue until the time when the grout reaches its maximum length of penetration,  $r_g$ , in all joints (Figure 16f). Connecting the locations of  $r_g$  in all joints to each other produces a 3-D space in the form of a cylinder. This is the exact time when the operation is finished.

The general case is the one in which a multiple joint sets, each with specific parameters of aperture, spacing, and persistence, cross the rock mass at differing angles. The grouting process in this case is similar to the case of one joint set such that the grout starts to fill the borehole and the joints from the lower part of the section. Almost all joints with a proper groutability will be grouted if the process is continued but the length of penetration would be different based on their aperture. Thus the length of grout penetration in the case of multiple joint sets can still be calculated using Equations (14) and (17).

In practice, however, the grouting might have various uncertainties and complications, thus causing variations in the results from what were predicted. For example, occurrence of the bleeding phenomenon may be responsible for deterioration

in the quality of the process. Additionally, a poor design or genuine geological complications can be hard on the quality of the operation. These can result in an asymmetrical space around the borehole in which the quality may not be similar in different locations. Although one area is not grouted only with one borehole, it is necessary to obtain the best quality of grouting around each borehole, and this highlights the significance of not only a suitable grout but a proper pattern of the boreholes. An optimum design is of paramount importance financially as well, for the distance between the boreholes largely dictates the drilling extent the amount of material used, and operation time. According to what mentioned above, there are two crucial points regarding grouting: 1) selection of suitable grout based on the project conditions and 2) prediction of grout propagation in the region being grouted. The present part of this paper concentrates on the latter point.

The reliable space that has been grouted properly is a space in which all joints are filled with the grout. Therefore, the length of penetration for the whole borehole will be determined after calculating the length of penetration for each joint. In many cases, it might equal the smallest length of penetration in the smallest joint aperture, given that the joint does not have a small persistence. Nonetheless, it does not hold true for all conditions. Generally, it is suggested that the borehole spacing is chosen based on not only the penetration in major joints but the *in situ* conditions and the goal of grouting.

## 7. Discussion

In the present work, a mathematical model for prediction of the length of grout penetration in rock joints was proposed. The joint apertures according to the ISRM classification [86] was selected, and the technical parameters were chosen according to

the previous studies and experience obtained by the other researchers [14, 87]. As it could be seen, in both the horizontal and angled cases, the joint aperture has a relation with the length of grout penetration. The values obtained for the joints with larger apertures grouted by grouts with ratios of 1:1 and 2:1 are too large, which are not technically acceptable. According to Shroff and Shah [14], the multiple grouting stages are performed to compensate it, particularly for the apertures larger than 6 mm. With this strategy, the grout can fill the joints efficiently with controllable penetration lengths. Another technique can use thicker grouts.

Higher grouting pressures increase the length of penetration inside the joints. This strategy has been proposed by many researchers in order to achieve the maximum length of grout penetration in rocks, and it can be much greater for the grouts with higher water to cement ratios. The ratios used in the present work are the most usual ones in the rock improvement.

In the angled case, shown in Figures 8 and 9, when 0.5:1 ratio is used, the increase in the angle gives rise to decreases equal to 1 cm and 5 cm for aperture 2.5 mm and 10 mm, respectively. According to Figures 10 and 11, the values for the 1:1 ratio will be 25 cm and 1 m, respectively, and Figures 12 and 13 show that they will be 60 cm and 2.4 m. To sum up, for a specific water to cement ration, as the joint aperture increases, the decrease in the length of penetration rises for a horizontal joint. Additionally, with water to cement ration increasing, the difference between the values of the length of penetration of angled and horizontal increases. This is of importance for the design of a proper distance between the boreholes.

All in all, the equations presented in the present paper give the length of penetration in the horizontal and angled single joints. It was shown that these equations were applicable for the multiple joints case under all circumstances.

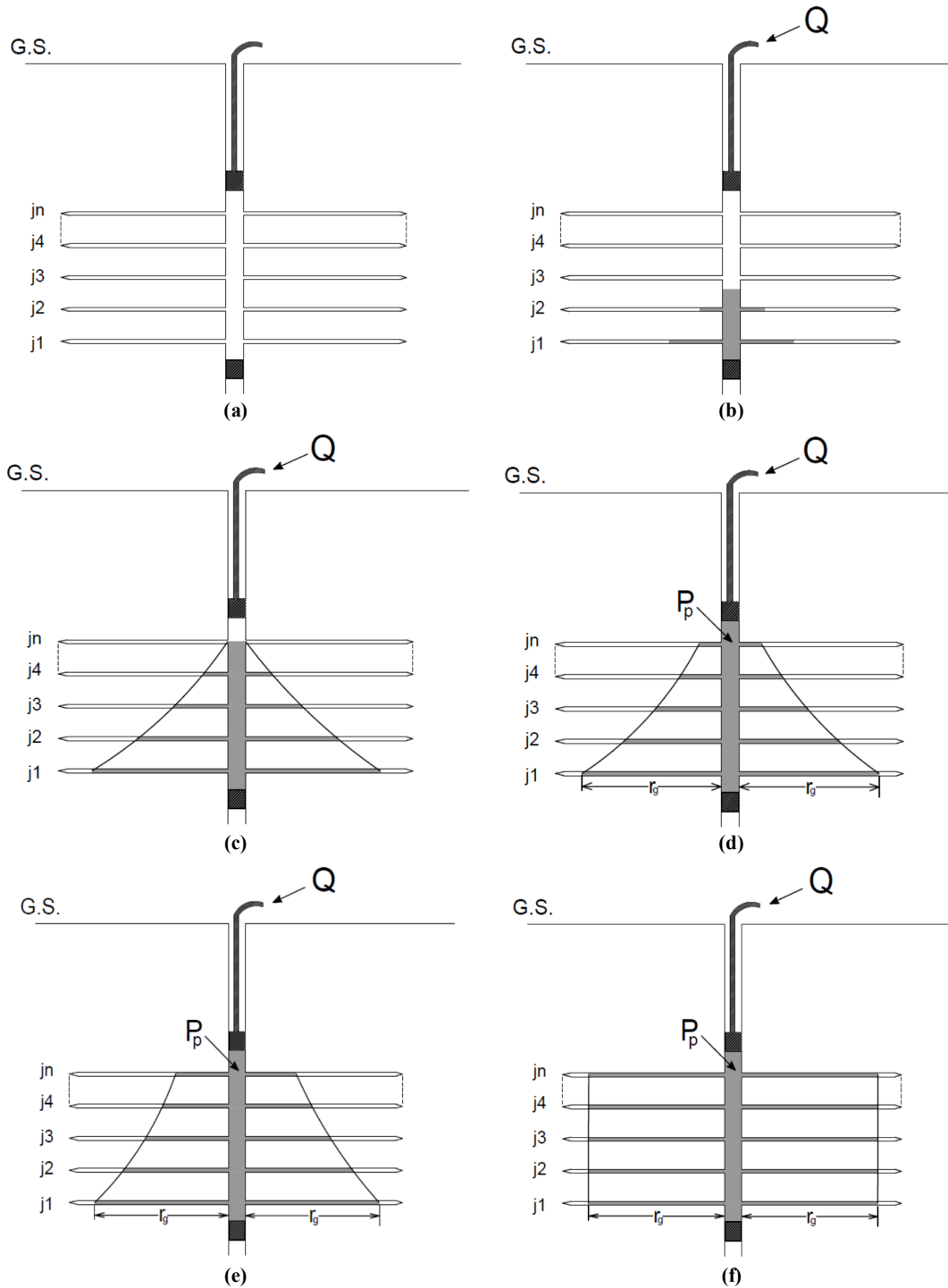


Figure 16. Grouting process in one joint set with n horizontal joints.

### 8. Comparison of results with current empirical criteria

Empirically, the only criteria available would be comparison of the spacing and groutability of boreholes in the joints with different apertures. After investigations on many grouting projects, Evert [89] has proposed that relatively closed joints

(apertures smaller than 0.5 mm) show little intake, and the grout propagation will be a few centimeters, while joint hydraulic apertures greater than 1 mm show high intake levels and the length of penetration could be between 1 m to 10 m. These are in accordance with the results of the equations in the present work for a grout pressure of 1 bar.

Furthermore, according to the bodies of experience attained for the design of boreholes distance [90], the distance for low apertures (closed to relatively closed joints) would be between 1 m and 3 m, and for open to large voids, it could be between 4 m and 15 m. The values calculated in the present research work are comparable to these suggested distances. From Figure 5, it is inferred that for a joint with an aperture of 2 mm, the length of penetration could change from 2 m to 5 m depending on the pressure. Thus to achieve the necessary overlap, the distance between the boreholes has to be in the range of 4 m-10 m, which is in accordance with the current empirical proposed values.

### 9. Comparison of present methods developed with existing related formulas

The previous researchers based their formulas on different assumptions and conditions, so there are specific parameters in each of them, some of which may be found only in one formula. Thus comparison of the values from the equations proposed in the present work will be made with those of the existing formulas, which include similar parameters. The formula proposed by Jiakai *et al.* [11] includes the grouting time, which is incomparable to the equations proposed in this paper. The formula proposed by Shroff and Shah [14] includes the grout volume, while the other formulas including Equations (14) and (17) do not include it. There are many parameters in the formula obtained by Majdi *et al.* [15], two of which are the depth of the joint and grouting time. This again limits the comparison of this formula with those proposed by the present paper. Therefore, Equation (14) is to be compared with the formulas proposed by Wittke [9], Lombardi [12], and Lau and Crawford [13] for a grout with a water to cement ratio of 1:1 and a grouting pressure of 6 bar. Table 4 presents the values of the length of penetration obtained from all these equations.

As it can be seen, the values obtained from the formulas proposed by Wittke and Lombardi are very large and unrealistic since these formulas are based on the pipe model assumed for joints, which is not a suitable model for the planar structure of the joints. The values obtained from the formula

proposed by Lau and Crawford are larger than those obtained from Equation (14) for the apertures smaller than 3 mm. For larger apertures, both formulas present similar values (Figure 17). This is due to consideration of shear distribution in the present work, which can affect the results for the small apertures. Lau and Crawford have simulated the joint with two glass plates, thus ignoring the friction between the grout and the joint walls. Consequently, the results of the equations proposed in the present work are more realistic and reliable even for the joints with small apertures.

### 10. Case study

The Nosoud water conveying tunnel is part of the huge project of conveying water to the tropical plains of western Iran, which conveys Sirvan river water to the arable lands located in the south part of the Kermanshah province. The Leyleh part is the southern part of this tunnel, which is situated in the Javanroud county, is 6 km long, and has a conveying capacity of 70 m<sup>3</sup>/s. The drilling diameter and the final diameter equal 6.12 m and 5.4 m, respectively. The engineers who worked in this project encountered various challenges, the most important of which were water inrush and sulfur gas leakage. In order to cure water inrush, the grouting technique was proposed.

The grouting method was crucial in this project because:

- 1) The drilling diameter achieved using TBM was larger than the prefabricated lining, so it was necessary to apply the contact cement grouting to fill the space between the lining and the rock. This changes a discrete region into a seamless region, resulting in smaller deformations and prevention of water inrush.
- 2) This tunnel passes through fault zones and highly jointed rock masses, and this causes water permeation and inrush. Thus contact grouting would not be so efficient, dictating the necessity of supplementary grouting.
- 3) The tunnel had a negative dip, complicating the water prevention and drilling operations due to water accumulation in front of the tunnel face. Figure 18 shows water inrush in the Nosoud tunnel.

**Table 4. Comparison of length of grout penetration obtained from Equation (14) and those obtained from the existing formulas**

Aperture (mm)	Present work (m)	Wittke (m) [9]	Lombardi (m) [12]	Lau and Crawford [13] (m)
0.1	0.044	20.727	20.689	0.849
0.25	0.131	51.762	51.724	1.364
0.5	0.698	103.486	103.448	1.945
1.0	2.235	206.934	206.896	2.766
1.5	3.159	310.382	310.344	3.396
2.0	3.807	413.831	413.793	3.927
2.5	4.331	517.279	517.241	4.395
3.0	4.785	620.727	620.689	4.818
4.0	5.567	827.624	827.586	5.570
5.0	6.244	1034.520	1034.482	6.231
6.0	6.850	1241.417	1241.379	6.830
7.0	7.405	1448.313	1448.275	7.380
8.0	7.920	1655.210	1655.172	7.892
9.0	8.403	1862.106	1862.068	8.373
10.0	8.860	2069.003	2068.965	8.828

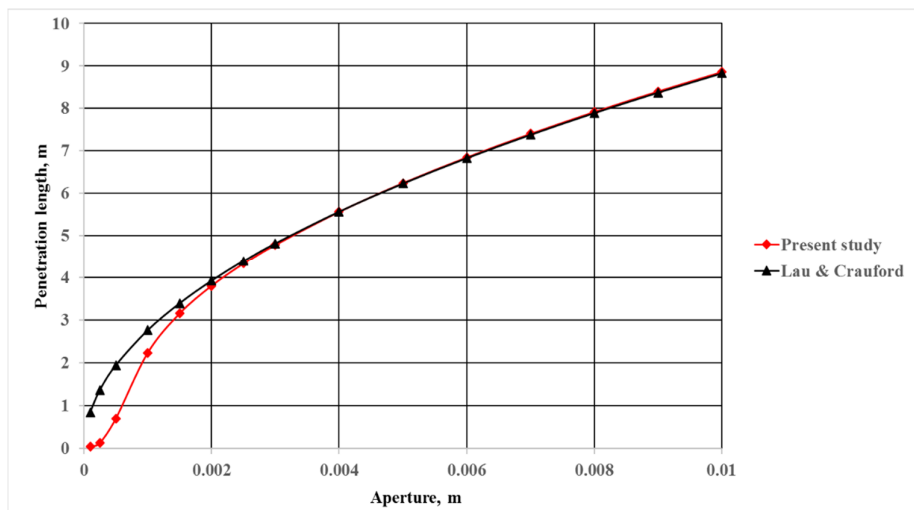


**Figure 17. Comparison of length of penetration values predicted by Lau and Crawford [13] and those calculated by Equation (14) for a horizontal joint.**



**Figure 18. Inrush water in Nosoud tunnel.**

A relatively thick grout was selected to fill the vacant spaces, due to large extent of these regions as well as the need for a suitable grout with admirable filling properties. The grout is a mixture of water, cement (type V), bentonite, and additives. Sieved sand was added as well.

Contact grouting should be performed by a gradual increase of pressure and decrease of grout use. Regarding the conditions, a grouting pressure of 4 bar was proposed. For supplementary grouting, a grouting pressure of 8 bar was suggested in order to fill the vacant regions completely without damaging the rock and the lining.

The joint apertures were all around 2 mm. From the equation proposed in the present work (Equation (17)), the length of grout penetration for the pressure of 4 bar was 1 m (Figure 4), which was perceived to create a suitable overlap of grout. Figure 19 shows the boreholes array on the tunnel section. The performance method was as follows:

- 1) To prevent grout loss, the segments on the tunnel floor were isolated.
- 2) Since the borehole array was designed according to segments dispositions, one of the adjacent segments was grouted. Therefore, boreholes 1 and 9 on the floor, 4 at the back of the ventilation duct, and 6 at the top of the conveyor belt were back-filled.
- 3) Segment joints were filled completely.
- 4) Grouting of the boreholes was performed on a ring pattern, from the top boreholes to the lower ones.
- 5) The grouting operation was stopped immediately after observing grout backlash.

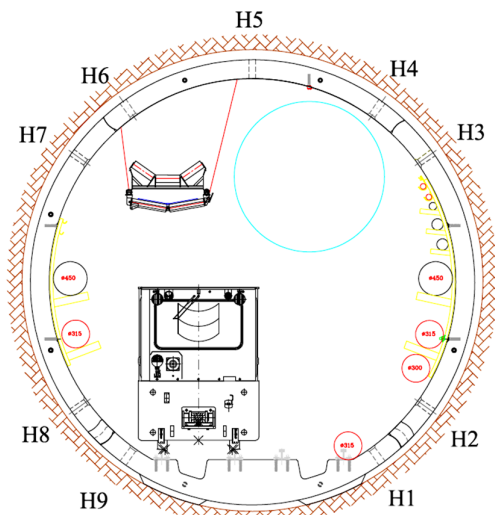


Figure 19. Borehole array on the tunnel section of Nosoud tunnel.

After performance of all the grouting steps, the admirable result was achieved such that not only was the grouting operation performed completely, the tunnel was sealed perfectly. It was shown that the analytical model proposed in the present study could predict the suitable design of the grouting operation. No points with water inrush or leakage were observed, and the space between the segment and the rock was filled ideally.

## 11. Conclusions

In the present paper, two analytical equations were proposed in order to calculate the length of grout penetration in the horizontal and angled rock joints. The joints were assumed as disks with infinite expansion in the space. The grout particle was assumed to be much finer than the joint aperture. The fluid was Binghamian, and its properties did not change during the operation. The length of penetration was calculated for three grout mixtures with water to cement ratios, which are usually applied for water sealing and rock consolidation. The calculations presented the following result.

- 1) The length of grout penetration increases with the joint hydraulic aperture. The values for a large aperture can be very high.
- 2) The grouting pressure could be a deciding factor in reaching the maximum length of penetration. The values used were the most usual ones applied in rock grouting.
- 3) In the angled joints, the length of penetration is in the two sides. The difference in the length of penetration between the horizontal and angled cases increases with water to cement ratio.
- 4) When the multiple joints intersect the borehole, the length of penetration in all the major joints should be calculated firstly, and then the smallest length can be chosen. It should be noted that the joints with small persistence might not be of significance.
- 5) The length of penetration in the upper part of angled joints should be taken into account.
- 6) It was shown that the equations proposed could be used to predict the length of penetration in the joints with unequal aperture values, thus not being limited to the single-joint case.
- 7) The values obtained from the present developed analytical model were compatible with the empirical criteria. They also could predict the proper design for sealing a water conveying tunnel.

The model proposed in the present work can be used to calculate the length of grout penetration not only in single joints but in rock masses with multitude crossing joints. Therefore, it may be useful when determining the distance between the grouting boreholes to ascertain a qualified grouting operation.

## References

- [1]. Jaeger, J.C., Cook N.G.W. and Zimmerman, R.W. (2007). *Fundamentals of Rock Mechanics*. Fourth Edition, Blackwell Publishing.
- [2]. Durham, W.B. and Bonner B.P. (1994). Self-propping and fluid flow experiments in slightly offset joints at high effective pressures. *J Geophysical Research: Solid Earth*, 99(B5), 9391-9.
- [3]. Makurat, A. and Gutierrez M. (1996). Fracture flow and fracture cross flow experiments, Paper 36732 presented at the 1996 SPE Annual Technical Conference and Exhibition. Denver, CO, October 6-9, 511-519.
- [4]. Zimmerman, R.W. and Bodvarsson, G.S. (1996). Hydraulic conductivity of rock fractures. *Transport in Porous Media*, 23, 1-30.
- [5]. Yeo, I.W., de Freitas M.H. and Zimmerman R.W. (1998). Effect of shear displacement on the aperture and permeability of a rock fracture. *International Journal of Rock Mechanics and Mining Sciences*, 35(8), 1050-70.
- [6]. Chen, Z., Narayan S.P., Yang Z. and Rahman, S.S. (2000). An experimental investigation of hydraulic behavior of fractures and joints in granitic rock. *International Journal of Rock Mechanics and Mining Sciences*, 37, 1061-1071.
- [7]. Barton, N. and de Quadros, E.F. (1997). Joint aperture and roughness in the prediction of flow and groutability of rock masses. *International Journal of Rock Mechanics and Mining Sciences*, 34(3-4), 252-e1.
- Weaver, K. D. (1991). *Dam foundation grouting*. American Society of Civil Engineers, New York, N.Y.
- [8]. Håkansson, U., Hässler, L. and Stille, H. (1992). Rheological properties of microfine cement grouts. *Tunnelling and Underground Space Technology*, 7, 453-458.
- [9]. Wittke, W. (1968). Zur Reichweite von Injektionen in klüftigen Fels. *Felsmechanik und Ingenieurgeologie Supplementum*, Volume IV, Springer, Wien-New York, 79-89.
- [10]. Wittke, W. (1990). *Rock Mechanics-Theory and application with case studies*. Springer, Verlag, Berlin.
- [11]. Jiakai, L., Baochang, W., Wenguang, C., Yuhua, G. and Hesheng, C. (1982). Polyurethane Grouting in hydraulic engineering. *Proceedings of conference of Grouting in Geotechnical Engineering*, New Orleans, W.
- H. Baker (editors) *American Society of Civil Engineering*, New York, 403-417.
- [12]. Lombardi, G. (1985). The role of cohesion in cement grouting of rock: 15th ICOLD Congress, Lausanne, III, 235-261.
- [13]. Lau, D. and Crawford, A. (1986, January). The Cement Grouting of Discontinuities in Rock Masses. In the 27th US Symposium on Rock Mechanics (USRMS). American Rock Mechanics Association.
- [14]. Shroff, A. V. and Shah, D. L. (1999). *Grouting Technology in Tunnelling and Dam Construction*. A. A. Balkema, Rotterdam, Brookfield.
- [15]. Majdi, A., Pourrahimian, Y. and Bagheri, H. (2004). Theoretical Prediction of Grout-Take in Jointed Rock Masses. *International Conference on Ground Improvement Techniques*, Kuala Lumpur, Malaysia, 237-244.
- [16]. Widmann, R. (1996, December). International society for rock mechanics commission on rock grouting. In *International journal of rock mechanics and mining sciences geomechanics abstracts* (Vol. 33, No. 8, pp. 803-847). Pergamon.
- [17]. Warner, J. (2004). *Practical handbook of grouting: soil, rock, and structures*. John Wiley and Sons.
- [18]. Draganovic, A. and Stille, H. (2011). Filtration and penetrability of cement-based grout: Study performed with a short slot. *Tunnelling and underground space technology*, 26(4), 548-559.
- [19]. Nonveiller, E. (1968, October). Grouted Cutoff Curtains in fissured rock. In *Rock Mechanics Symp Proc*, Madrid/Sp/.
- [20]. Verfel, J. (1989). *Rock grouting and diaphragm wall construction*. Elsevier, Amsterdam.
- [21]. Draganovic, A. and Stille, H. (2011). Filtration and penetrability of cement-based grout: Study performed with a short slot. *Tunnelling and underground space technology*, 26(4), 548-559.
- [22]. Baker, C. (1974). Comments on paper "Rock Stabilization in Rock Mechanics. Edited by L. Muller. Springer-verlag, Wien-New York. Literature during Course held at the Dept. of Mechanics of Solids, UDINE.
- [23]. Baghbanan, A. and Jing, L. (2007). Hydraulic properties of fractured rock masses with correlated fracture length and aperture. *International Journal of Rock Mechanics and Mining Sciences*, 44(5), 704-719.
- [24]. Cacas, M.C., Ledoux, E., de Marsily, G., Tillie, B., Barbreau, A., Durand, E., ... and Peaudecerf, P. (1990). Modeling fracture flow with a stochastic discrete fracture network: calibration and validation: 1. The flow model. *Water Resources Research*, 26(3), 479-489.
- [25]. Dershowitz, W., De, T., Uchida, M. and Hermanson, J. (2007). Analysis of groundwater inflow

control by grouting using the discrete fracture network method. *Felsbau*, 25(4), 34-41.

[26]. Cvetkovic, V. and Frampton, A. (2012). Solute transport and retention in three-dimensional fracture networks. *Water resources research*, 48(2).

[27]. Dessirier, B., Tsang, C. F. and Niemi, A. (2018). A new scripting library for modeling flow and transport in fractured rock with channel networks. *Computers and Geosciences*, 111, 181-189.

[28]. Dreuzy, J.R., Méheust, Y. and Pichot, G. (2012). Influence of fracture scale heterogeneity on the flow properties of three-dimensional discrete fracture networks (DFN). *Journal of Geophysical Research: Solid Earth*, 117(B11).

[29]. Hässler, L. (1991). Grouting of Rock-Simulation and Classification [PhD thesis]. KTH Royal Institute of Technology, Stockholm.

[30]. Nguyen, V. H., Rémond, S., Gallias, J.L., Bigas, J.P. and Muller, P. (2006). Flow of Herschel-Bulkley fluids through the Marsh cone. *Journal of non-Newtonian fluid mechanics*, 139(1-2), 128-134.

[31]. Balhoff, M., Sanchez-Rivera, D., Kwok, A., Mehmani, Y. and Prodanović, M. (2012). Numerical algorithms for network modeling of yield stress and other non-Newtonian fluids in porous media. *Transport in porous media*, 93(3), 363-379.

[32]. Rahman, M., Håkansson, U., and Wiklund, J. (2015). In-line rheological measurements of cement grouts: Effects of water/cement ratio and hydration. *Tunnelling and Underground Space Technology*, 45, 34-42.

[33]. Shamu, T. J. and Håkansson, U. (2019). Rheology of cement grouts: On the critical shear rate and no-slip regime in the Couette geometry. *Cement and Concrete Research*, 123.

[34]. Herschel, W.H. and Bulkley, R. (1926). Konsistenzmessungen von Gummi Benzollösungen. *KolloidZeitschrift* 39 (4), 291-300.

[35]. Håkansson, U. (1993). Rheology of Fresh Cement-based Grouts. Doctoral Thesis, Department of Infrastructure and Environmental Engineering. Division of Soil and Rock Mechanics, Royal Institute of Technology, Stockholm, Sweden.

[36]. Funehag, J. and Fransson, Å. (2006). Sealing narrow fractures with a Newtonian fluid: model prediction for grouting verified by field study. *Tunnelling and underground space technology*, 21(5), 492-498.

[37]. Lombardi, G. (2003). Grouting of rock masses. In: *International Conference on Grouting and Ground Treatment*, 164-197.

[38]. Hässler, L., Stille, H. and Håkansson, U. (1987). Simulation of grouting in jointed rock. In: *Proceeding of*

the Sixth International Congress on Rock Mechanics, Balkema, Rotterdam, 2, 943-946.

[39]. Hässler, L., Håkansson, U. and Stille, H. (1992). Computer-simulated flow of grouts in jointed rock. *Tunnelling and Underground Space Technology* 7(4), 441-446.

[40]. Mohajerani, S., Baghbanan, A., Bagherpour, R. and Hashemolhosseini, H. (2015) Grout penetration in fractured rock mass using a new developed explicit algorithm. *International Journal of Rock Mechanics and Mining Sciences*, 80, 412-417.

[41]. Eriksson, M., Stille, H. and Andersson, J. (2000). Numerical calculations for prediction of grout spread with account for filtration and varying aperture. *Tunnelling and Underground Space Technology*, 15(4), 353-364.

[42]. Janson, T. (1998). Calculation models for estimation of grout take in hard jointed rocks. Ph.D, Royal Institute of Technology.

[43]. Dalmalm T. (2001), Grouting Prediction systems for hard Rock-based on active design. Royal Institute of Technology, Stockholm, Sweden.

[44]. Dalmalm, T. (2004). Choice of grouting method for jointed hard rock based on sealing time predictions. Ph.D, Royal Institute of Technology.

[45]. Rahmani, H. (2009). Estimation of Grout Distribution in a Fractured Rock by Numerical Modeling. MSc Dissertation. Vancouver: The University of British Columbia.

[46]. Lee J.S., Bang C.S., Mok Y.J. and Joh, S.H. (2000). Numerical and experimental analysis of penetration grouting in jointed rock masses. *International Journal of Rock Mechanics and Mining Sciences*, 37(7), 1027-1037.

[47]. Hässler, L., Håkansson, U. and Stille, H. (1992). Classification of jointed rock with emphasis on grouting. *Tunnelling and underground space technology*, 7(4), 447-452.

[48]. Gustafson, G., Claesson, J. and Fransson, Å. (2013). Steering parameters for rock grouting. *Journal of Applied Mathematics*, 2013.

[49]. Gustafson, G. and Stille, H. (2005). Stop criteria for cement grouting. *Felsbau: Zeitschrift für Geomechanik und Ingenieurgeologie im Bauwesen und Bergbau*, 25(3), 62-68.

[50]. Kobayashi, S., Stille, H., Gustafson, G. and Stille, B. (2008). Real-time grouting control method. Development and application using Äspö HRL data (No. SKB-R--08-133). Swedish Nuclear Fuel and Waste Management Co.

[51]. Stille, B., Stille, H., Gustafson, G. and Kobayashi, S. (2009). Experience with the real time grouting control method. *Geomechanics and Tunnelling*, 2(5), 447-459.

- [52]. Lavrov, A. (2013). Numerical modeling of steady-state flow of a non-Newtonian power-law fluid in a rough-walled fracture. *Computers and Geotechnics*, 50, 101-109.
- [53]. Lavrov, A. (2015). Flow of truncated power-law fluid between parallel walls for hydraulic fracturing applications. *Journal of non-Newtonian Fluid Mechanics*, 223, 141-146.
- [54]. Bao, K., Lavrov, A. and Nilsen, H. M. (2016, August). Numerical Modelling of non-Newtonian Fluid Flow in Fractures and Porous Media. In *ECMOR XV-15th European Conference on the Mathematics of Oil Recovery* (pp. cp-494). European Association of Geoscientists & Engineers.
- [55]. Amadei, B. and Savage, W. Z. (2001). An analytical solution for transient flow of Bingham viscoplastic materials in rock fractures. *International Journal of Rock Mechanics and Mining Sciences*, 38, 285-296.
- [56]. Yang M.J., Yue Z.Q., Lee P.K., Su B. and Tham L.G. (2002). Prediction of grout penetration in fractured rocks by numerical simulation. *Canadian Geotechnical Journal*. 39(6), 1384-1394.
- [57]. Mortazavi A. and Maadikhah A. (2016). An investigation of the effects of important grouting and rock parameters on the grouting process. *Geomechanics and Geoengineering*, 1-17.
- [58]. Fidelibus, C. and Lenti, V. (2012). Short note: The propagation of grout in pipe networks. *Computers and Geosciences*, 45, 331-336.
- [59]. Rutqvist, J. and Stephansson O. (2003). The role of hydromechanical coupling in fractured rock engineering. *Hydrogeology Journal*, 11(1), 7-40.
- [60]. Zimmerman R. and Main, I. (2003). Chapter 7 hydromechanical behavior of fractured rocks. *Int Geophys.*, 89, 363-421.
- [61]. Tsang, C.F., Bernier F. and Davies, C. (2005). Geohydromechanical processes in the excavation damaged zone in crystalline rock, rock salt, and indurated and plastic clays—in the context of radioactive waste disposal. *International Journal of Rock Mechanics and Mining Sciences*, 42(1), 109-125.
- [62]. Gothäl, R. and Stille, H. (2009). Fracture dilation during grouting. *Tunnelling and Underground Space Technology*, 24, 126-135.
- [63]. Lecampion, B. (2009). An extended finite element method for hydraulic fracture problems. *Communications in Numerical Methods in Engineering*, 25(2), 121-133.
- [64]. Gupta, P. and Duarte, C.A. (2014). Simulation of non-planar three-dimensional hydraulic fracture propagation. *International Journal for Numerical and Analytical Methods in Geomechanics*, 38(13), 1397-1430.
- [65]. Marina, S., Derek, I., Mohamed, P., Yong, S. and Imo-Imo, E.K. (2015). Simulation of the hydraulic fracturing process of fractured rocks by the discrete element method. *Environmental earth sciences*, 73(12), 8451-8469.
- [66]. Lei, Q., Latham, J.P. and Tsang C.F. (2017). The use of discrete fracture networks for modelling coupled geomechanical and hydrological behavior of fractured rocks. *Computers and Geotechnics*, 85, 151-176.
- [67]. Yan, X., Sun, Z. and Dong, Q. (2021). The unified pipe-interface element method for simulating the coupled hydro-mechanical grouting process in fractured rock with fracture propagation. *Engineering Fracture Mechanics*, 256, 107993.
- [68]. Yan, C., Tong, Y., Luo, Z., Ke, W. and Wang, G. (2021). A two-dimensional grouting model considering hydromechanical coupling and fracturing for fractured rock mass. *Engineering Analysis with Boundary Elements*, 133, 385-397.
- [69]. Gothall, R. and Stille, H. (2009). Fracture dilation during grouting. *Tunnelling and Underground Space Technology*, 24(2), 126-135.
- [70]. El Tani, M. and Stille, H. (2017). Grout spread and injection period of silica solution and cement mix in rock fractures. *Rock Mechanics and Rock Engineering*, 50(9), 2365-2380.
- [71]. Kim, H.M., Lee, J.W., Yazdani, M., Tohidi, E., Nejati, H.R. and Park, E.S. (2018). Coupled viscous fluid flow and joint deformation analysis for grout injection in a rock joint. *Rock Mechanics and Rock Engineering*, 51(2), 627-638.
- [72]. Sun, L., Grasselli, G., Liu, Q. and Tang, X. (2019). Coupled hydro-mechanical analysis for grout penetration in fractured rocks using the finite-discrete element method. *International Journal of Rock Mechanics and Mining Sciences*, 124, 104138.
- [73]. Rutqvist, J. and Stephansson, O. (1996). Acyclic hydraulic jacking test to determine the in situ stress normal to a fracture. *International Journal of Rock Mechanics and Mining Sciences*, 33(7), 695-711.
- [74]. Rafi, J.Y. and Stille, H. (2014). Control of rock jacking considering spread of grout and grouting pressure. *Tunnelling and Underground Space Technology*, 40, 1-15.
- [75]. Ghafar, A.N., Montesidis, A., Draganovic, A. and Larsson, S. (2016). An experimental approach to the development of dynamic pressure to improve grout spread. *Rock Mechanics and Rock Engineering*, 49(9), 3709-3721.
- [76]. Rahman, M., Wiklund, J., Kotzé, R. and Håkansson, U. (2017). Yield stress of cement grouts. *Tunnelling and Underground Space Technology*, 61, 50-60.

- [77]. Gustafson G. and Stille, H. (1996). Prediction of groutability from grout properties and hydrological data. *Tunnelling and Underground Space Technology*, 11, 325-32.
- [78]. Xu, Z., Liu, C., Zhou, X., Gao, G. and Feng, X. (2019). Full-scale physical modelling of fissure grouting in deep underground rocks. *Tunnelling and Underground Space Technology*, 89, 249-261.
- [79]. Liu, Q., Sun, L. and Tang, X. (2019). Investigate the influence of the in-situ stress conditions on the grout penetration process in fractured rocks using the combined finite-discrete element method. *Engineering Analysis with Boundary Elements*, 106, 86-101.
- [80]. Zou, L., Håkansson, U. and Cvetkovic, V. (2018). Two-phase cement grout propagation in homogeneous water-saturated rock fractures. *International Journal of Rock Mechanics and Mining Sciences*, 106, 243-249.
- [81]. Zou, L., Håkansson, U. and Cvetkovic, V. (2020). Yield-power-law fluid propagation in water-saturated fracture networks with application to rock grouting. *Tunnelling and Underground Space Technology*, 95, 103170.
- [82]. Lee, J. S., Sagong, M., Park, J. and Choi, I. Y. (2020). Experimental analysis of penetration grouting in umbrella arch method for tunnel reinforcement. *International Journal of Rock Mechanics and Mining Sciences*, 130, 104346.
- [83]. Wang, X., Xiao, F., Zhang, Q., Zhou, A. and Liu, R. (2021). Grouting characteristics in rock fractures with rough surfaces: Apparatus design and experimental study. *Measurement*, 184, 109870.
- [84]. Shamu, T.J., Zou, L. and Håkansson, U. (2021). A nomogram for cement-based rock grouting. *Tunnelling and Underground Space Technology*, 116, 104110.
- [85]. Rafi, J. and Stille, H. (2021). A method for determining grouting pressure and stop criteria to control grout spread distance and fracture dilation. *Tunnelling and Underground Space Technology*, 112, 103885.
- [86]. ISRM, International Society for Rock Mechanics, (1982). Suggested Methods for rock characterization, Testing and Monitoring, *International journal of Rock Mechanics & Mining Science & Geomechanical Abstracts*.
- [87]. Kutzener, C. (1996). Grouting of rock and soil. 271 pages (p. 4-8), A. A. Balkema.
- [88]. Majdi, A. and Mirzazade, A. (2017, August). Prediction of Minimal Rock Mass Grouting Pressure based on Newton's Second Law and Principles of Fracture Mechanics. In 51st US Rock Mechanics/Geomechanics Symposium. American Rock Mechanics Association.
- [89]. Ewert, F.K. (1985). Rock grouting with emphasis on dam sites. 428P. Springer-Verlag, Berlin.
- [90]. Leblais, Y. (2005). Ground reinforcement for tunneling in weak ground. ITA/AITE Straining Course Tunnel Engineering, Istanbul.

## ارائه یک روش تحلیلی به منظور پیش‌بینی طول نفوذ آمیزه تزریق در سنگ‌های درزه‌دار

محمد مهدی ناظم‌پور و عباس مجدی\*

دانشکده مهندسی معدن، پردیس دانشکده‌های فنی، دانشگاه تهران، ایران

ارسال ۲۰۲۱/۱۲/۱۲، پذیرش ۲۰۲۲/۰۱/۱۰

\* نویسنده مسئول مکاتبات: amajdi@ut.ac.ir

---

### چکیده:

پیش‌بینی طول نفوذ آمیزه تزریق و ارزیابی تزریق‌پذیری در اطراف گمانه‌های تزریق در سنگ‌های درزه‌دار اثر مهمی بر طراحی و اجرای عملیات تزریق دارد. توزیع آمیزه تزریق در سنگ‌های درزه‌دار تابعی از ویژگی‌های ژئومکانیکی توده‌سنگ، ویژگی‌های آمیزه تزریق و پارامترهای اجرایی تزریق می‌باشد. مقاله پیش رو یک مدل تحلیلی مبتنی بر قانون دوم نیوتن را توصیف می‌کند که با فرض درزه‌های دیسک شکل، حداکثر طول نفوذ آمیزه تزریق را در درزه‌های افقی و زاویه‌دار محاسبه می‌کند. نشان داده شد که فرمول‌های پیشنهادی قادر هستند طول نفوذ آمیزه تزریق را در توده‌سنگ‌های دارای چندین دسته درزه نیز محاسبه کنند. به منظور اعتبارسنجی، مدل پیشنهادی با معیارهای تحلیلی و تجربی موجود مقایسه شد که نتایج تطابق خوبی با یکدیگر داشتند. نهایتاً، مدل پیشنهادی برای طراحی تزریق در یک تونل انتقال آب که در معرض هجوم آب شدید قرار داشت، به کار رفت. این طراحی منجر به پر شدگی مناسب فضای خالی پشت سگمنت و آب‌بندی تونل شد که نتیجه آن توقف آب ورودی به تونل بود. نتایج نشان دادند که مدل پیشنهادی در این مقاله می‌تواند به طور موفقیت آمیزی در عملیات اجرایی نیز به کار رود.

**کلمات کلیدی:** سنگ‌های درزه‌دار، درزه‌های سنگی، قانون دوم نیوتن، سیال بینگه‌امی، طول نفوذ آمیزه تزریق.

---